Steel Reinforcement Ratio Dependency of Plastic Rotational Capacity of Reinforced Concrete Beams

Walid M. Hasan [1], Moh'd El-Khatieb [2] and Hamid Al-Ani [3]

[1] Assistant Professor, Department of Civil Engineering, Al-Isra University, Amman, Jordan,
E-mail: walid.hasan@ iu.edu.jo
[2] Assistant Professor, Department of Civil Engineering, Al-Isra University, Amman, Jordan
[3] Associate Professor, Department of Civil Engineering, Al-Isra University, Amman, Jordan

ABSTRACT

This paper describes experimental observations intended to verify the dependency of plastic rotational capacity on steel reinforcement ratio.

Variable parameters are: scale, steel ratio and slenderness. Experimental results are obtained varying the percentage of reinforcement and beam dimensions to analyze the structural response for a practical construction. These beams are normally designed in such a way that the internal forces as well as their distribution over the transversal section are calculated using the elastic beam theory, while the beam dimensions are designed using the ultimate limit state. Reinforced concrete beams must be designed to have a ductile response. This is necessary to guarantee the structural safety and internal forces redistribution during their life. In fracture mechanics, it is seen that beams with higher dimensions are brittle, while those with small dimensions are ductile. So, it is important to clarify whether the same material and design concepts can be applied for reinforced concrete beams with different dimensions. The influence of size and steel ratio on the inelastic rotational capacity has not been completely clarified and demonstrated yet. In fact, the experimental data available up to a few years ago, mostly obtained by load-controlled tests on reinforced concrete beams with high ductility bars, show a considerable scatter. On the other hand, some numerical evaluations, assuming strain localization in the compression zone, indicate that plastic rotation depends on the steel ratio and scale (beam depth), and the experimental tests recently carried out seem to validate this dependence.

KEYWORDS: Minimum reinforcement, Brittleness number, Fracture mechanics, Transitional failure phenomenon, Plastic rotation.

INTRODUCTION

Reinforced concrete beams undergo different failure mechanisms by varying beam slenderness and/or reinforcement ratio and/or beam size-scale. The three fundamental collapse mechanisms are the following:

- Formation of inclined shear cracks;

- Compression and crushing at the edge in compression;
- Nucleation and propagation of cracks at the edge in tension.

Regarding the tensile failures, the minimum amount of reinforcement can be determined through the concepts of fracture mechanics, while the maximum inelastic rotational capacity can be obtained even when failure shifts to the compressive side. Many

experimental tests confirmed that both such quantities are subjected to remarkable size effect. It is well known that the minimum reinforcement (minimum amount of steel which prevents brittle failure) must be sufficient to absorb the tension forces present in the concrete immediately before failure. In other words, the minimum percentage of reinforcement must guarantee that when the tension resistance of concrete has been overpowered, it is still possible to meet more stable response of the same beam. According to some studies (Ozbolt and Bruckner, 1999), based on fracture mechanics, it was revealed that the minimum reinforcement depends on beam dimensions, in contrast with design codes, where the minimum reinforcement is independent of the dimension h, Fig. 1.
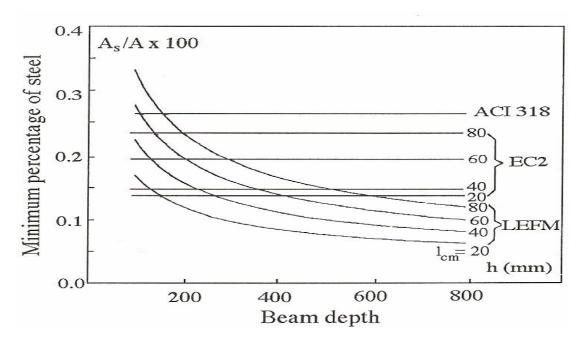

Figure 1: Minimum percentage of steel *versus* beam depth

One of the ways to express the ductility of a reinforced concrete beam is the ultimate plastic rotation. As a rule, this is defined as the inelastic rotation in correspondence with the ultimate bending moment. Assuming the usual constitutive law of steel and concrete, the maximum moment is reached for lower values of curvature. With more realistic assumption, the peak value would be achieved for further curvature. In the following analysis, we compute the ultimate rotation values in correspondence with a relative curvature at a moment equal to 90% of the peak value of the descending branch.

The rotation obtained in this way has been purified from the elastic value assumed in correspondence with the yield strength of reinforcement.

The test has been conducted until failure with displacement control, for a percentage of steel reinforcement greater than 0.25, and a deflection control is used for values less or equal to 0.25.

The result of a non-linear analysis depends on the project values assumed for the material properties in the different parts of the structure.

Without considering the second order effect and considering the non-linear behavior of the material and the tension stiffening, the code (CEB, 1993) indicates that for the position of the load assumed, the mean value

of the material properties remains invariant until the yielding value of the steel has been reached in the critical section. Once this limit is reached, for the material properties, the calculated value must be

assumed in correspondence with the critical section and the maximum capacity is assumed to be equal to the one at the ultimate limit state.
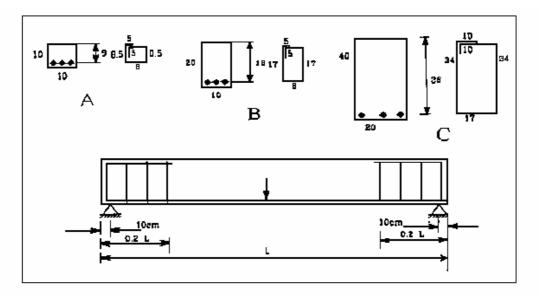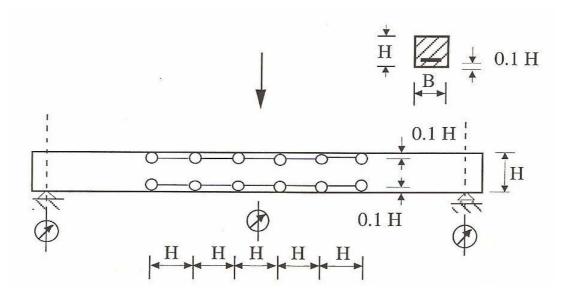

Figure 2: Beam reinforcement detail

Figure 3: Setup of transducers

Figure 4: Bending moment *versus* plastic rotation diagrams of beams of type A (100 x 100 mm) with a slenderness ratio equal to 18 and various steel ratios

Figure 5: Bending moment *versus* plastic rotation diagrams of beams of type B (100 x 200 mm) with a slenderness ratio equal to 6 and various steel ratios
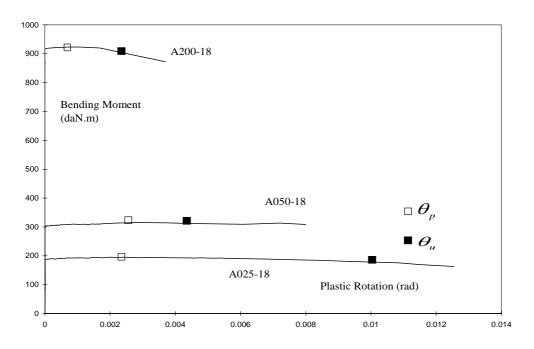
Figure 6: Bending moment *versus* plastic rotation diagrams of beams of type B (100 x 200 mm) with a slenderness ratio equal to 12 and various steel ratios
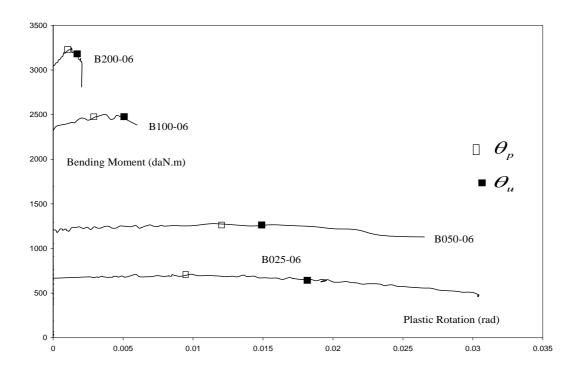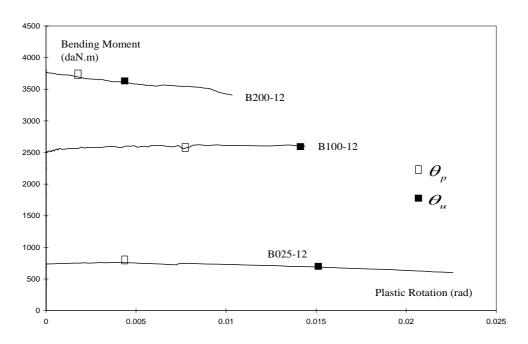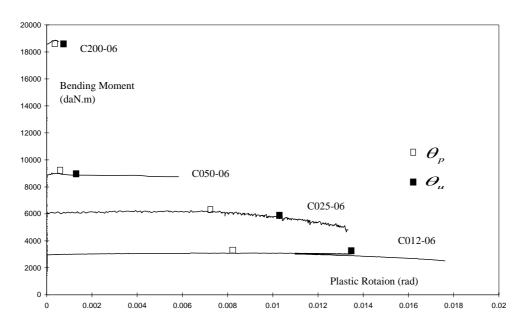

Figure 7: Bending moment *versus* plastic rotation diagrams of beams of type C (200 x 400 mm) with a slenderness ratio equal to 6 and various steel ratios

The critical sections are localized in correspondence with the peak value of the bending moment through the zones, where these characteristics have the same sign. In absence of the axial force and with a constitutive law of

the steel elastic-plastic hardening, it is possible to assume, when the yielding point of steel is reached, that the critical sections act like plastic hinges up to the ultimate moment value, while the plastic rotation reaches its ultimate value.

The model indicated corresponds to assume a third segment of the constitutive law of the section, defined in a reference of translated system with origin in the yielding point of steel, in which its inclination is defined as the ratio between the difference of the ultimate moment values and the permitted plastic rotation as mentioned above.

It is interesting to note that in presence of a high percentage of steel reinforcement, large deformations of concrete occur before the steel yields. In this case, the above consideration must be modified even if, from a general point of view, we can make reference to the constitutive law with three segments.

Experimental Details

Three point bending test on 17 reinforced concrete beams were performed. The beams were divided into classes A, B and C with cross-sectional area $b \times h$ equal to 100×100, 100×200 and 200×400 mm, respectively, with different steel ratios, 0.125, 0.25, 0.50, 1.00 and 2.00% (for main steel and stirrups arrangement, see Fig. 2), and different slenderness values (l/h span to depth ratio) of 6, 12 and 18. The beams were tested in the Laboratory of the Structural Engineering Department of Turin University. The testing machine used was a closed-loop servo-controlled machine. The tests were performed in displacement-controlled conditions to be able to record the descending branch of the load-displacement curve, if any. The displacement transducers employed to control the loading process were placed at mid span on the lower edge of the specimen. The measuring range was greater than the maximum expected specimen deflection at failure, so as to avoid signal resisting; for transducer rearrangement (see Fig. 3 and Fig 8). The values of the experimental parameters of the beams are reported in Table 1.

Theoretical Model

The plastic rotation is formally expressed as a unique function of the ratio x/d between the neutral axis depth and the useful depth of the beam without ignoring that this ratio is related to the reinforcement ratio, while recent studies have also considered the steel ductility effect (Lounis et al., 2010). The influence of steel ductility, in fact, has become important because of the technological evolution of steel production, which reduces the ratio f_t / f_y with respect to the past.

On the other hand, the plastic behavior of the reinforced concrete structures is very influenced by other factors like:

- The confinement conditions in the compression zone of the beam section;
- The bond conditions between steel bars and concrete;
- The bending moment gradient;
- The scale effect;
- Test procedure;
- The area of the contact zone between the implicated load and the beam surface.

Concerning the definition, the plastic rotation has no unique definition, but it's always related to the calculation method adapted to the structural analysis.

In indeterminate structure, the definition used is that given in (CEB, 1993). The plastic rotation θ_p will be obtained by integration along the plastic zone l_p (where the stress in the tension steel is greater than its yielding limit) as the difference between the total curvature $1/r_m$ and the curvature obtained at the limit of the yielding point of steel $1/r_{my}$ as follows:

$$\theta_p = \int_{lp} (1/r_m - 1/r_{my})dz \qquad (1)$$

In equation (1), the curvatures are obtained from the rotation between the difference of the average strain of the tension line ε_{sm} and the compression one ε_{cm} which corresponds to the signed value of the transducers located at $h/10$ from the upper and lower edges of the beam section as follows:

$$1/r_m = (\varepsilon_{sm} - \varepsilon_{cm})/0.8h \qquad (2)$$

where h is the depth of the cross-section of the beam.

The ultimate rotation θ_u is measured in correspondence with the 90% of the maximum moment in the descending branch, before failure.

If this value is not reached, so the value in correspondence with failure will be assumed.

The ultimate load p_u is obtained from the experimental results with the same criteria adopted for the ultimate rotation.

Table 1. Characteristic loads, deflection and rotations of the tested beams

Beam	Yielding load p_y (kN)	Peak load p_p (kN)	Ultimate load p_u (kN)	Mid-span deflection at peak load δ_p (mm)	Plastic rotation at peak load θ_p	Ultimate rotation θ_u
A100-06	3843	3910	3519	6.10	1.250 E-2	4.210 E-2
A200-06	6154	6276	5648	7.23	1.020 E-2	3.993 E-2
A025-18	366	376	339	14.40	2.380 E-3	1.082 E-2
A050-18	628	642	578	22.60	2.860 E-3	4.400 E-3
A200-18	1936	1994	1795	16.80	1.070 E-3	3.700 E-3
B025-06	2170	2295	2065	5.18	8.910 E-3	1.790 E-2
B050-06	3947	4185	3766	7.13	1.131 E-2	1.510 E-2
B100-06	7674	8300	7470	12.57	4.310 E-3	6.340 E-3
B200-06	9946	10753	9678	5.18	1.060 E-3	1.630 E-3
B025-12	1118	1134	1021	12.40	4.000 E-3	1.544 E-2
B100-12	4163	4236	3812	40.00	8.510 E-3	1.439 E-2
B200-12	6173	6223	5600	36.70	3.620 E-3	5.000 E-3
C012-06	4546	4665	4198	8.64	8.225 E-3	1.346 E-2
C025-06	9594	9869	8882	12.65	7.315 E-3	1.086 E-2
C050-06	14262	14527	13074	8.10	2.310 E-4	7.000 E-4
C200-06	30459	30954	27858	10.03	4.030 E-4	5.320 E-4
C050-18	4007	4037	3633	49.20	3.670 E-3	4.000 E-3

The Relation between Bending Moment and Rotation

The rotation due to the applied load is given by the effect of superposition as follows:

$$\Delta\varphi = \lambda_{mm}M - \lambda_{mp}p \tag{3}$$

where $\lambda_{mm} = \dfrac{2}{h^2 bE}\displaystyle\int_0^{\xi} Y_M^2(\xi)d\xi$ and

$\lambda_{pp} = \dfrac{2}{bE}\displaystyle\int_{c/h}^{lo} y_p^2(c/h,\zeta)d\zeta$ referred to relative depth

ζ of the crack.

Let us consider $\Delta\varphi_f$ a local rotation due to the presence of the crack when the applied bending moment reaches its value M_f (the bending moment value at first crack), so it is possible to define the local rotation $\Delta\varphi_{f0}$ for an initial depth related to the crack ζ_0 at the crack propagation. When $M = M_f$, equation (1) becomes:

$$\Delta\varphi_f = \lambda_{mm}M_f - \lambda_{mp}p\alpha \tag{4}$$

where $\alpha = M_f/M_p = P/P_p < 1$ if $M_f < M_p$ (bending moment which corresponds to the yielding point of steel) and $\alpha = 1$ if $M_f \geq M_p$.

Equation (3) could be expressed as a function of the

geometrical parameters of the cracked element, for this reason, assuming the stress intensification factor equal to the critical one $K_1 = K_{1c}$, where

$$K_1 = \frac{M}{h^{1.5}b}Y_M(\xi) - \frac{P}{h^{0.5}b}Y_p(c/h,\xi) \text{ if } M < M_p \text{ and}$$

$$K_1 = \frac{M}{h^{1.5}b}Y_M(\xi) - \frac{P_p}{h^{0.5}b}Y_p(c/h,\xi) \text{ if } M > M_p. \text{ We}$$

get:

$$K_{1c} = (M_F / h^{1.5}b)Y_M(\xi) - (P/h^{0.5}b)Y_p(c/h,\xi). \quad (5)$$

Considering $P = P_p\alpha$ yields:

$$M_f = \frac{K_{1c}h^{1.5}b}{Y_M(\xi)} + \frac{Y_p(c/h,\xi)}{Y_M(\xi)}P_ph\alpha \qquad (6)$$

Using the above expression, equation (2) becomes:

$$\Delta\varphi_f = \lambda_{mm}\left[\frac{K_{1c}h^{1.5}b}{Y_m(\xi)} + \frac{Y_p(c/h,\xi)}{Y_m(\xi)}P_ph\alpha\right] - \lambda_{mp}P_p\alpha. \quad (7)$$

Recalling the relation (Bosco and Carpinteri, 1992):

$$r(c/h,\xi) = \frac{\displaystyle\int_{c/h}^{\xi}Y_M(\xi)Y_p(c/h,\xi)}{\displaystyle\int_0^\xi Y_M^2(\xi)d\xi} = \frac{\lambda_{MP}}{\lambda_{MM}h} \qquad (8)$$

and considering the brittleness number (Carpinteri, 1981), $N_p = \dfrac{f_yh^{0.5}}{K_{IC}}A_s / A$, equation (7) becomes:

$$\Delta\varphi_f = \lambda_{MM}\frac{K_{IC}bh^{1.5}}{Y_M(\xi)}\{1 + [Y_p(c/h,\xi) - \qquad (9)$$

$$r(c/h,\xi)Y_M(\xi)]N_P\alpha\}$$

In this equation, we have always to consider $\alpha < 1$ if $M_f < M_p$ and

$\alpha = 1$ if $M_f \geq M_p$. From equation (6), considering

$M_p = P_phr'(c/h,\xi)$, we get:

$$\alpha = M_f / M_p = \frac{K_{1c}bh^{1.5}}{P_phY_M(\xi)r'(c/h,\xi)} + \frac{Y_P(c/h,\xi)M_F}{Y_M(\xi)r'(c/h,\xi)M_P}. \qquad (10)$$

Rearranging the above equation, we get:

$$M_f / M_P\left[1 - \frac{Y_P(c/h,\xi)}{r'(c/h,\xi)Y_M(\xi)}\right] = \frac{1}{N_Pr'(c/h,\xi)Y_M(\xi)} \qquad (11)$$

where $N_P = P_ph /(K_{1c}bh^{1.5})$, and finally we get:

$$\alpha = M_f / M_P = \frac{1}{[Y_M(\xi)r'(c/h,\xi) - Y_P(c/h,\xi)]N_P}$$

for $M_f < M_p$ \qquad (12)

and

$\alpha = 1$ for $M_f \geq M_p$.

From equations (10) and (12), it is possible to obtain the relation between the unitless rotation $\Delta\varphi_F / K_{1c}bh^{1.5}$ and the brittleness number N_P (Carpinteri, 1981) for a certain depth of the relative crack ξ. On the other hand, it is possible to consider the ratio $\Delta\varphi_F / \Delta\varphi_{F0}$ between the values given from equation (6) for $\xi > \xi_0$, respectively as an X-coordinate of the diagram, where $M_f / K_{1c}bh^{1.5}$ is the Y - coordinate in this case. In fact, if the crack propagation is seen as an evaluative phenomenon, the parameter ξ gives the correspondent position of the crack mouth. The dimensionless bending moment diagram in relation with the rotation could be obtained till the point in which the crack produces the complete separation of the section.

So, for a certain geometry and tenacity, the constitutive behavior of the cracked section is well interpreted by the brittleness number N_P. This is

exactly the same conclusion, which has been found when congruence in terms of rotation (Bosco and

Carpinteri, 1992) has been adopted.

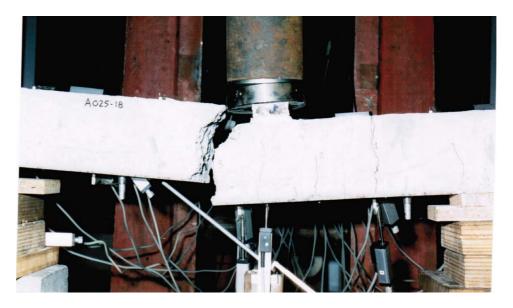**Figure 8: Test set-up of beam B100-12**

Figure 9: Brittle failure of beam A025-18

Brittle or Ductile Collapse

For a practical goal, it is important to find out the point in which the M_f (the bending moment value at first crack) reaches M_p (bending moment which corresponds to the yielding point of steel). This condition helps us determine the minimum percentage

of reinforcement which guarantees the beam resistance.

From equation (3), it is possible to write:

$$\Delta\varphi = \lambda_{mm}(M - M_p) \text{ for } M > M_p . \qquad (13)$$

Such linear tendency will stop when the crack propagation starts.
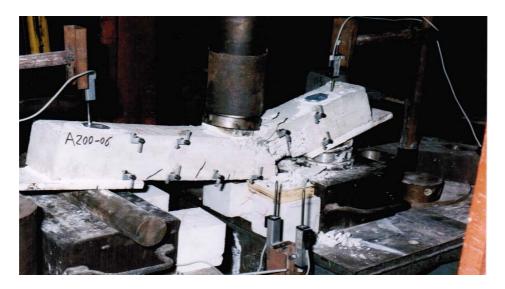
Figure 10: Concrete crushing failure of beam A200-06 with high steel ratio

Figure 11: Shear failure of beam 100-12

At this point, if the fracture phenomenon is unstable, the relation $M - \Delta\varphi$ presents a discontinuity and its value will correspond to the complete separation of the ligament.

If the fracture phenomenon is stable, the discontinuity will vanish and continuous hardening response will be obtained (Carpinteri, 1984).

Experimental Results

The plastic rotation *versus* bending moment curves are shown in Figs. 4 to 7, where slenderness and cross-section have been maintained constant varying the percentage of reinforcement. The comments here are applied to beams of type B.
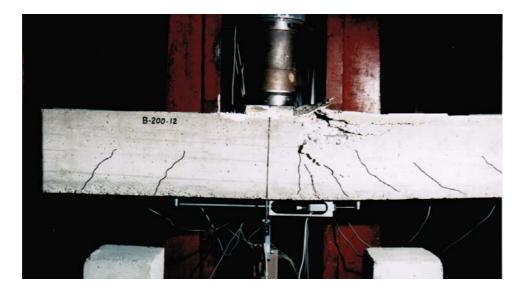
Figure 12: Compression failure of beam B200-12

Beams of type B with a slenderness value equal to 6 are represented in Fig. 5. It is easy to observe the different ductility values shown by the four beams; for B025-06 and B050-06 in particular, the plastic rotation is higher with respect to the values of the other two beams. It should be noted that in the first three beams the plastic rotation is calculated at 90% of the applied load in the descending branch of the load-displacement curve, while beam B200-06 shows that the crushing of concrete in the compression zone took place before reaching the 90% of the peak load. In this last case, we detect that the plastic rotation is practically negligible. On the other hand, with reference to equation (8), the plastic rotation becomes zero even if it appears due to the concrete deformation. In this case, a conventional value of the permanent deformation of the load-displacement diagram could be defined and again the plastic rotation could be obtained from equation (8).

CONCLUSIONS

From the diagrams shown in Figs. 4 to 7 and Table 1, it is necessary to emphasize that the plastic rotation decreases when increasing the steel ratio. This way of describing this phenomenon is equivalent to what has been indicated by CEB, where the plastic rotation expression is related to the depth of the neutral axis x at the ultimate limit state and the total depth of the beam d. The same observations could be indicated for the other tested beams as shown in Figs. 4 to 7. The difference in ductility, shown by the curves, is very clear and again confirms that the plastic rotation value decreases when the percentage of reinforcement increases.

The values of the experimental parameters, which describe the above comments, are shown in Table 1.

REFERENCES

American Concrete Institute. 2008. *Building Code Requirements for Structural Concrete and Commentary (ACI 318M-08)*, Detroit, Michigan.

Bigaj, A. and Walraven J. 2002. Size Effects in Plastic Hinges of Reinforced Concrete Members. *Heron*, 47(1): 53-75.

Bosco, C. and Carpinteri, A. 1992. Fracture Behaviour of Beam Cracked Across Reinforcement. *Theoretical and Applied Fracture Mechanics*, 17: 61-68.

Carpinteri, A., Ferro, G., Bosco, C. and El khatieb, M. 1999. Scale Effects and Transitional Failure Phenomena of Reinforced Concrete Beams in Flexure. *Minimum Reinforcement in Concrete Members*, Elsevier Science, Amsterdam, 1-30, Edited by Carpinteri, A.

Carpinteri, A., Corrado, M., Mancini, M. and Paggi, M. 2009. Size-Scale Effects on Plastic Rotational Capacity of Reinforced Concrete Beams. *ACI Structural Journal*, 106: 887-896.

Carpinteri, A. and Corrado, M. 2010. Dimensional Analysis Approach to the Plastic Rotation Capacity of Over-Reinforced Concrete Beams. *Engineering Fracture Mechanics*, 77(7): 1091-1100.

Carpinteri, A. 1981. A Fracture Mechanics Model for Reinforced Concrete Collapse. *IABSE Colloquium on Advanced Mechanics of Reinforced Concrete*, Delft University of Technology, Delft, The Netherlands, 34: 17-30.

Carpinteri, A. 1984. Stability of Fracturing Process in R.C. Beams. *Journal of Structural Engineering*, *ASCE*, 110: 544-558.

Comite' Euro-International du Beton (CEB). 1993. CEB-FIP Model Code 1990, Thomas Telford Services Ltd., London.

Corrado, M., Paggi, M. and Carpinteri, A. 2010. Limits to Plastic Analysis due to Size-Scale Effects on the Rotational Capacity of Reinforced Concrete Cross-Sections. *Structural Engineering International*, 20: 240-245.

Gamino, A.L., Sousa, J.L.A.O. and Bittencourt, T.N. 2008. Structural Dependence of Plastic Rotation Capacity in RC Beams. *Proceedings of the 8th World Congress on Computational Mechanics (WCCM8), 5th European Congress on Computational Methods in Applied Sciences and Engineering (ECCOMAS 2008)*, June 30 - July 5, Venice-Italy.

Karihaloo, B.L. 1995. Fracture Mechanics and Structural Concrete. Longman House, United Kingdom.

Kheyroddin, A. and Naderpour, H. 2007. Plastic Hinge Rotation Capacity of Reinforced Concrete Beams. *International Journal of Civil Engineering*, 5 (1): 30-47.

Ko, M.-Y., Kim, S.-W. and Kim, J.-K. 2001. Experimental Study on the Plastic Rotation Capacity Reinforced High Strength Concrete Beams. *Materials and Structures*, 34: 302-311.

Lounis, Z., Zhang, J.Y. and Almansour, H. 2010. Design of Long Life Concrete Structures Using High Performance Reinforcing Steels. *Proceedings of the 3rd Congress of the International Federation for Structural Concrete (FIB) and PCI Convention*, Washington, D.C., 1-10.

Ozbolt, J. and Bruckner, M. 1999. Minimum Reinforcement Requirement for RC Beams. *European Structural Integrity Society*, 24: 181-201.

Tada, H., Paris, P. and Irwin, G. 1963. The Stress Analysis of Cracks Handbook. Del Research Corporation, St. Louis, Missouri, Part 2, 16-17.